3D UNSTEADY CFD SIMULATION OF THE PRESSURE FLUCTUATION IN A CENTRIFUGAL FAN

Yang YANG, Andreas LUCIUS, Gunther BRENNER

Clausthal University, Institute of Applied Mechanics, Adolph-Roemer-Straße 2A, D-38678 Clausthal-Zellerfeld, Germany

SUMMARY

The purpose of the present study is to quantify pressure fluctuations in a high performance centrifugal fan. Since these fluctuations are causing severe dynamic loads, their assessment is crucial during the design process in view of life time prognoses. Using Computational Fluid Dynamics (CFD), the three dimensional unsteady flow field in the whole domain of impeller and volute casing is investigated. The calculations of the impeller with traditional spiral volute and a collection volute in combination with a vaneless diffuser are carried out for the design-point. Compared to the traditional spiral volute, the pressure fluctuation is considerably reduced through the application of the vaneless diffuser and collection volute. Further simulations for the new configuration show that the fluctuation in the impeller depends strongly on the flow rate.

INTRODUCTION

Centrifugal fans usually consist of a spiral volute casing to collect the flow. Due to the asymmetric shape of the volute/tongue in combination with the rotation of the impeller high dynamic loads are induced. This is in particular crucial since in centrifugal fans usually welded structures are used. This type of production is in general more sensitive to vibrations compared to casted constructions. Thus, during the design process and in view of life time prognoses the accurate prediction and assessment of these loads is of great importance. Due to that, the investigation of unsteady flows and flow instabilities in turbomachinery was subject to intensive research work in the past, both experimentally and numerically. Chen and Soundra-Nayagam [3] examined the unstable inlet vortex behavior in an industrial centrifugal fan experimentally. The pressure at different positions was measured with fast response pressure transducers. They found, that the pressure fluctuations are not influenced by the rotor speed but the flow rate. The instability caused by the inlet vortex is strong in the impeller inlet region and decreases downstream. Beside the vortex inlet, rotating stall has shown to be existent by Chen [4]. Both phenomena were clearly distinguished since the rotating stall only occurred below a critical flow rate. Madhavan and Wright [10] have shown the existence of rotating stall on the pressure side of the rotor, which occurs at very high flow rates. Khelladi [5] studied a centrifugal fan with a high rotational velocity numerically and experimentally. The

calculated overall performance, the variation of the pressure at a point on the impeller-diffuser interface with time and the static pressure distribution in impeller channel are in agreement with experiments. Ng [6] used computational flow models to analyze the performance of industrial fans with single and double inlet configurations. Ballesteros [7] studied the wall pressure fluctuation at the volute of an industrial centrifugal fan. Compared to the experimental data the numerical results show a good agreement. Majidi [8] calculated the flow field in a centrifugal pump. With investigation of nodal points, he found that the pressure fluctuation is strong at the impeller outlet and in the tongue region, due to the interaction between impeller and volute. Feng [5] investigated the pressure fluctuation for different configurations of vaned diffuser pumps. Increasing the radial gap between the impeller and the diffuser decreases the amplitude of the pressure fluctuations and the impeller-diffuser interactions are reduced significantly.

The present paper focuses on the unsteady flow field with reduced impeller volute interaction in a centrifugal fan. The pressure fluctuations in the ventilator with spiral volute and with collection volute in combination with vaneless diffuser is numerically investigated at optimal flow rate to understand the influence of the impeller volute interaction. For the configuration with diffuser and collection volute the further effect of flow rate is analysed. The paper is organized as follows: In the following section, the geometry and boundary condition of the two configurations will be described. In the next step the applied numerical model and the mesh generation will be introduced. At the end of this paper the results from the simulation will be discussed.

CENTRIFUGAL FAN AND OPERATIONAL CONDITIONS

The configurations of the centrifugal fan with traditional spiral volute and parallel vaneless diffuser considered in this paper are shown in Figure 1. Both designs represent typical industrial machines. The impeller with fifteen backswept blades is shrouded. It has an outlet diameter of 800 mm. To reduce the impeller volute interaction, a diffuser with an outlet diameter of 1160 mm is used to increase the distance between the impeller outlet and the tongue. The collection volute has a square cross-section. The shape of the collection volute is designed for a constant average velocity through all sections along the circumference.

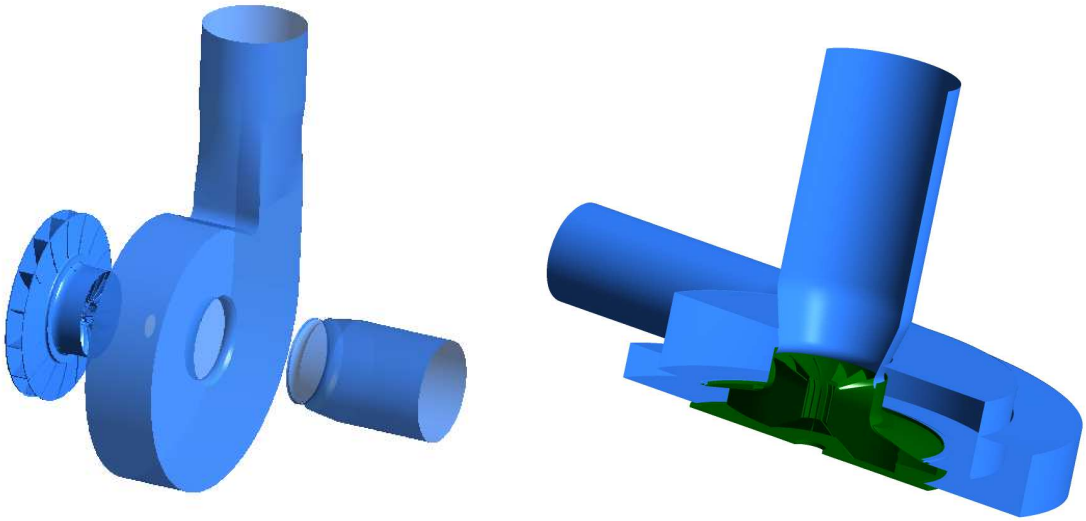

Figure 1: Configuration of the centrifugal fan, traditional spiral volute (left), diffuser with collection volute (right)

The impeller is designed for rotational speed as 3223 rpm and mass flow rate as 19.2 kg/s ($\dot{m}_{opt}$). For the configuration with diffuser and collection volute the pressure fluctuation at off-design points (50% $\dot{m}_{opt}$ and 150% $\dot{m}_{opt}$) will be investigate to obtain the influence of the flow rate.

COMPUTATIONAL MODEL AND MESH GENERATION

The numerical calculations in the present work have been performed with the commercial code ANSYS CFX 13.0. To resolve the time variation of the flow instabilities and unsteadiness, time resolving calculations are required. Thus, special attention has to be paid for the turbulence modelling. Turbulence resolving model such as LES in general would be able to account for the interaction between large scale flow instabilities and turbulence. However, due to the extremely high computational effort of these models for the present flow regimes, these models are prohibitive. Thus, an approach based on the Unsteady Reynolds-Average Navier-Stokes equation (URANS) is chosen. The SST [1] model is commonly applied for general purpose applications; it is often used in turbomachinery applications. The Scale-Adaptive Simulation (SAS) by Menter [1] may be regarded as a compromise between URANS and LES as it allows resolving turbulent fluctuations in parts of the boundary layer. As a compromise between effort and increased accuracy hybrid LES RANS models like DES (Detached Eddy Simulation) are increasingly used in unsteady flow computations. These models switch between RANS mode in stable flow regimes like attached boundary layers to LES mode in unstable regions of the computational domain. This leads to a significantly reduced size of the model compared to LES especially in turbulent boundary layers. The SAS model is chosen for the computations. It behaves much like the more common DES, but does not involve the grid size for switching from LES to RANS. The detection of unstable regions is done by the model itself by inclusion of the von Karman length scale. In these regions the eddy viscosity is reduced, allowing the development of large scale turbulent structures.

As has been shown in [2] for the flow in a part loaded pump, the SAS and SST models result in similar results as far as the pressure- and velocity distribution is considered. However, the spectra of the pressure fluctuations from simulation with the SAS model clearly show a better agreement with experimental results. Thus, in the present simulations the SAS model is chosen. A steady state solution was used as initial condition. The discretization in time is realized with a second order implicit integration scheme and a time increment corresponding to 300 steps per revolution. With this time step one blade pitch is calculated with 20 steps. The average Courant number is under 10 and the root mean square residual reaches 10^{-5} in the transient simulation. Due to the influence of the initial condition, three revolutions were needed to reach periodically stable result. After that, two further revolutions were simulated to obtain the transient flow field.

The computational domain included a stationary inlet pipe and casing, a rotating impeller and a stationary volute. The casing from the inlet domain connects the booth gap on the impeller shroud side. A jet flow develops through the inlet gap between the impeller and casing to improve the flow character along the curved shroud. The domains of inlet and impeller have a block structured grid. With O- and C-grid topologies the mesh can be matched with the geometry to achieve a satisfying quality. These topologies can be used in the traditional spiral volute also. Due to the topology of the geometry at the tongue and on the outlet side in the domain with diffuser and collection volute, it is virtually impossible to use a block structured grid in the whole outlet domain. For this reason, the domain in the vicinity of the tongue and the outlet is meshed with tetra elements and prism layers close to the wall. The remaining domain of the volute is meshed using a block structured grid. Three different mesh resolutions applied to determine the influence of the mesh size on the solution. The total pressure coefficient ψ was calculated as follow:

$$\psi = \frac{\Delta p_{tot}}{\frac{1}{2}\rho u^2} \tag{1}$$

Δp_{tot} is the total pressure rise, ρ is the density, u is the circumferential velocity at the rotor trailing edge. The result of the analysis is shown in Figure 2. The steady state computations show minor difference between the medium and high mesh resolution in both cases. Because of the huge

computational effort for the transient simulation, the medium mesh was chosen as compromise between mesh independence and the computational time. The grid for the configuration with spiral volute has 15 million nodes. The other configuration contains 13 million nodes. Figure 3 shows the computational grid.

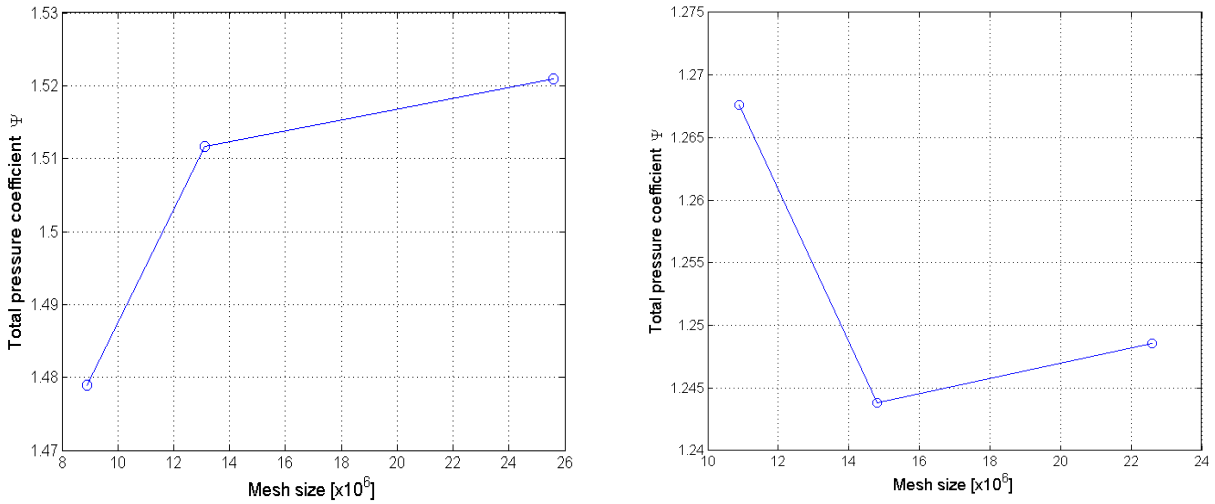

Figure 2: Influence of the mesh size on the solution, collection volute with diffuser (left) and spiral volute (right)

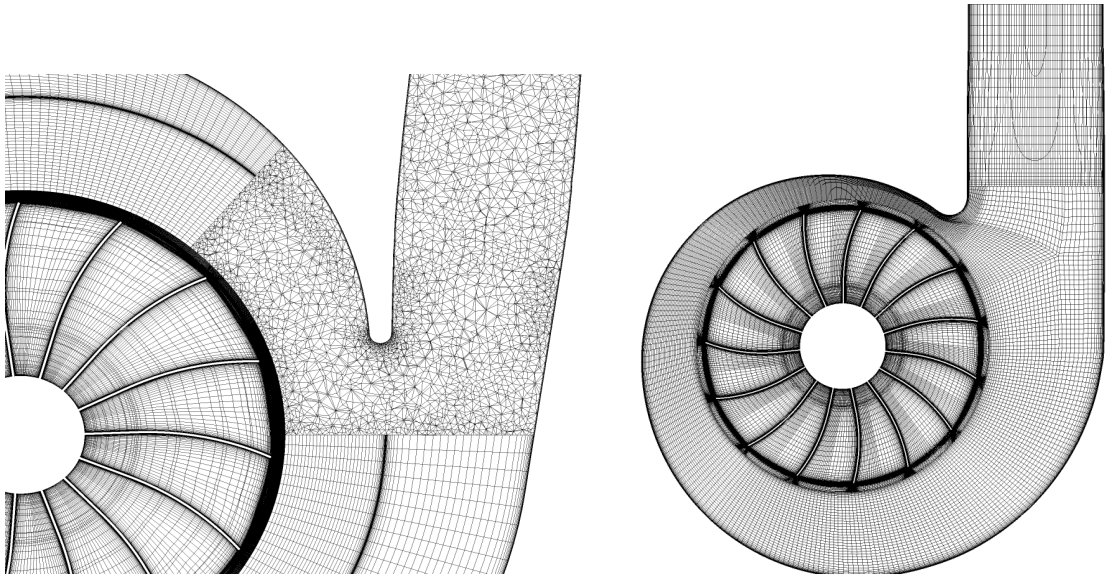

Figure 3: Grid of collection volute with diffuser (left) and spiral volute (right)

To connect the domains the General Grid Interface (GGI) is used. It allows non matching meshes on both sides of the interface in relative motion. Balance equations for the variable on the control surface within the interface region are generated from the flux contribution on both sides. In the case of relative motion, the relative position of each side is calculated first. As figure 4 shows, it provides the possibility of using different mesh type in one simulation and implements the mesh motion in a concise way.

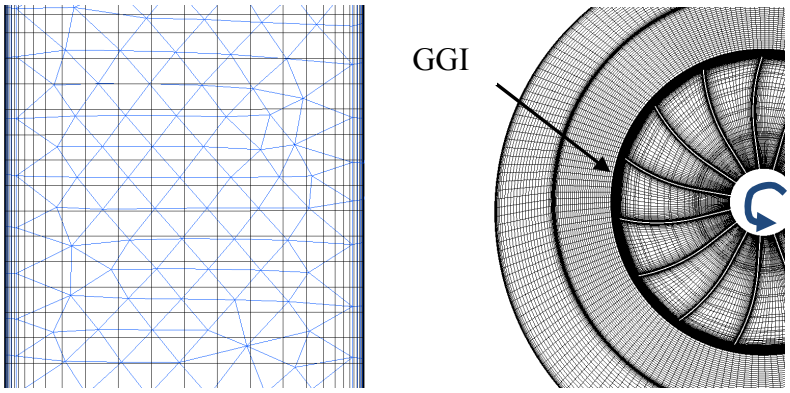

Figure 4: No matching mesh (left) and relative Movement of the mesh (right)

RESULTS AND DISCUSSIONS

In the following, the results of the calculations are discussed. Figure 3 shows the static pressure field at the median surfaces of both configurations. The tongue of the volute creates a geometrical asymmetry which influences the pressure distribution. Because of the short clearance between the impeller and volute tongue, strong interaction exists in the ventilator with spiral volute at design point. The interaction leads to a pressure fluctuation in the vicinity of the tongue and a non-uniform pressure distribution in impeller (Figure 5 left). With increasing distance between impeller and volute tongue, the effect of interaction is obviously reduced.

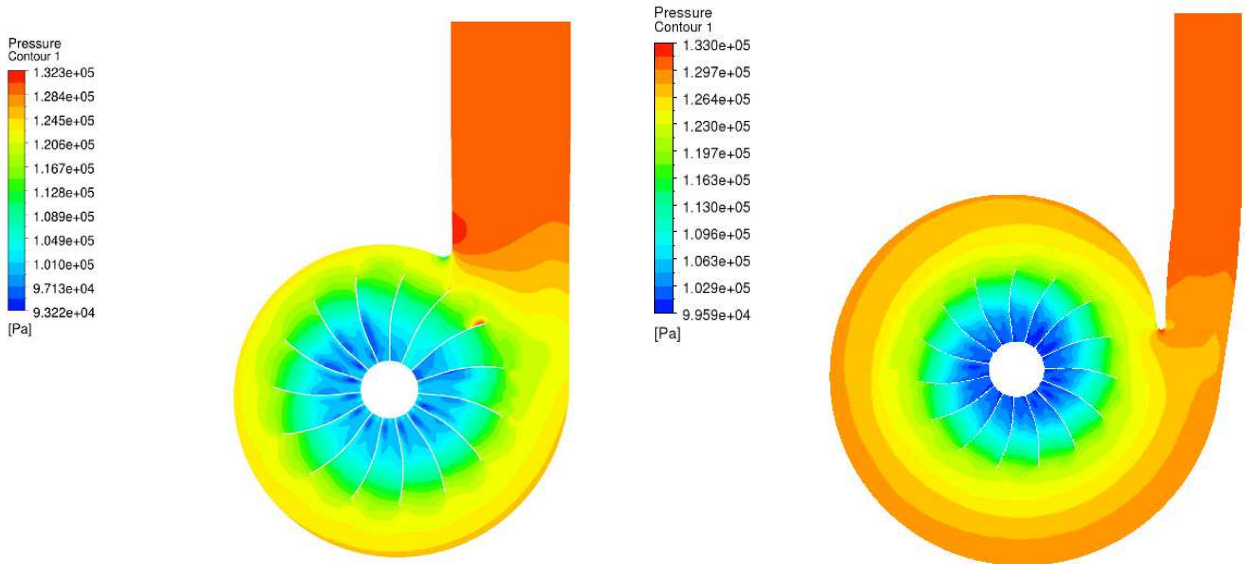

Figure 5: Pressure distribution at the meridian surface, 100% $\dot{m}_{opt}$

The total pressure coefficient over two revolutions obtained from the transient simulations is shown in figure 6. The ventilator with spiral volute presents a change of total pressure rise with rotational frequency at design point. With application of a diffuser, the fluctuation is considerably reduced except for the 50% part load case. The Fourier analysis was done with the Fast Fourier Transform (FFT) supplied by MATLAB. Figure 7 displays the result. The fluctuation of total pressure rise from the ventilator with spiral volute exhibits a good periodicity with the rotational and blade pass frequency. The rotor – volute interaction strongly influence the total pressure rise of the ventilator. The same effect is observed in the other configuration at design point. Considering the volute as a stator with one blade, the rotational frequency corresponds with the stator frequency. In both configurations the stator frequency dominant the total pressure rises at design point.

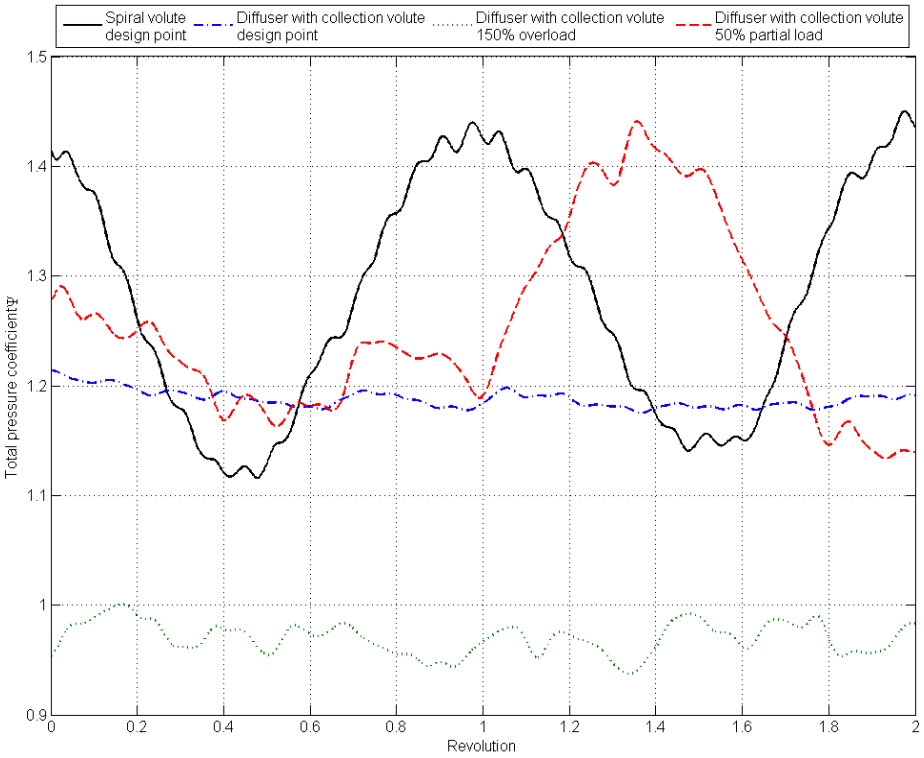

Figure 6: Change of Total pressure coefficient over the revolution

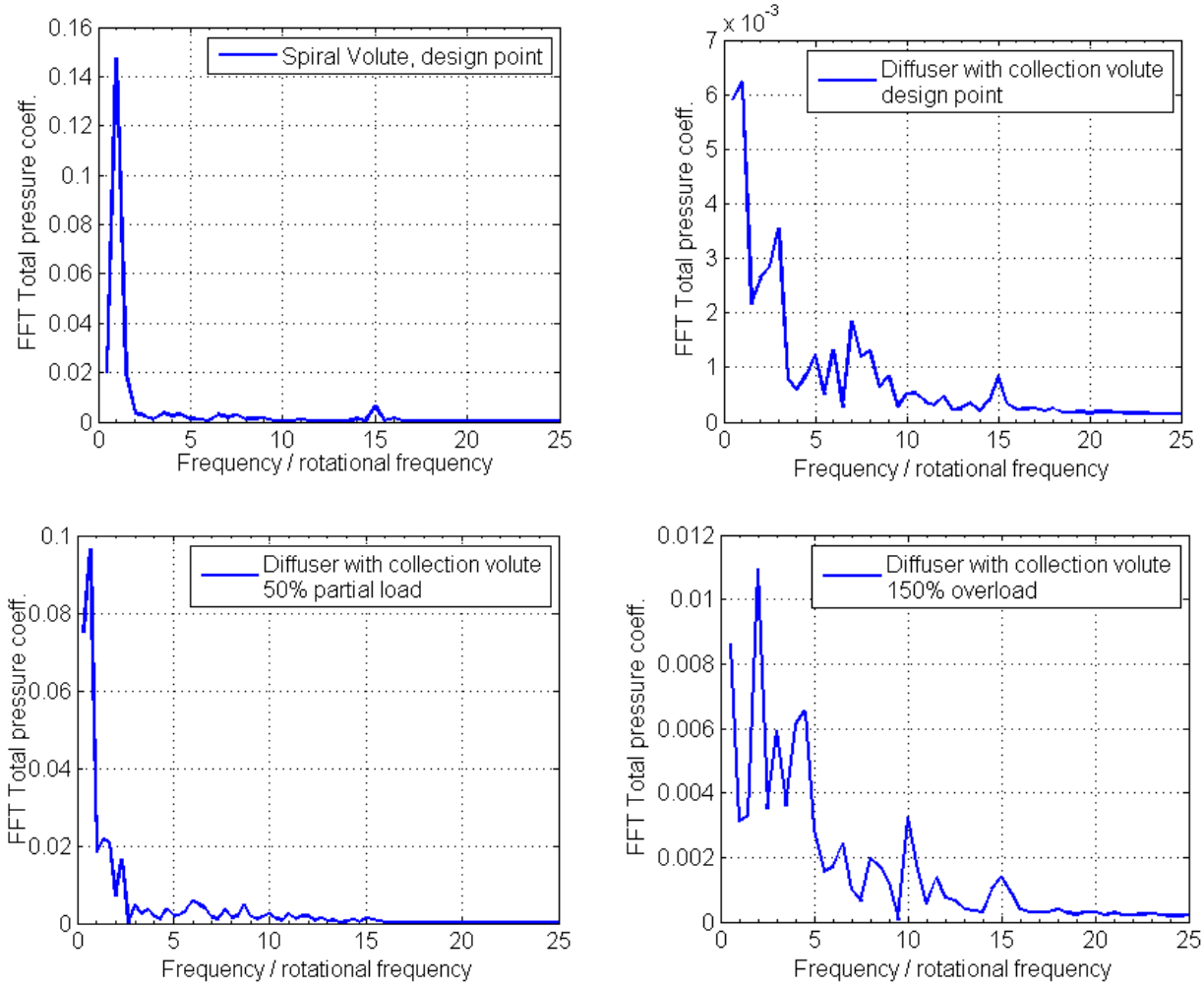

Figure 7: FFT Analysis of the total pressure coefficient

However, the amplitudes of pressure fluctuation are much smaller compared to the configuration with spiral volute. At 50% part load the relationship between the interaction and the fluctuation of total pressure rise cannot be seen, because stall cells are engendered by partial load, which dominant the flow field with a lower frequency as the one caused by rotor – spiral interaction. At the over load operating point the predominant frequency is twice of the rotational frequency. The amplitude of the fluctuation at high flow rate is much smaller than at partial flow rate. Both the predominant frequency and the amplitude depend on the flow rate.

To obtain an overview of the instability in the whole flow field, the change of pressure within the ventilator during the time was recorded. For the flow in the volute, the pressure data along the middle channel surface were considered. For the impeller flow field, the pressure along a surface in the middle between two blades is considered in rotating coordinates. On these surfaces, the amplitude of pressure is visualized in Figure 8. Considering the volute domain high amplitudes are observed in the vicinity of the tongue. As the flow changes its direction from axial to radial in the impeller, the pressure fluctuation reaches its maximum, which is over three times higher than the one in the volute.

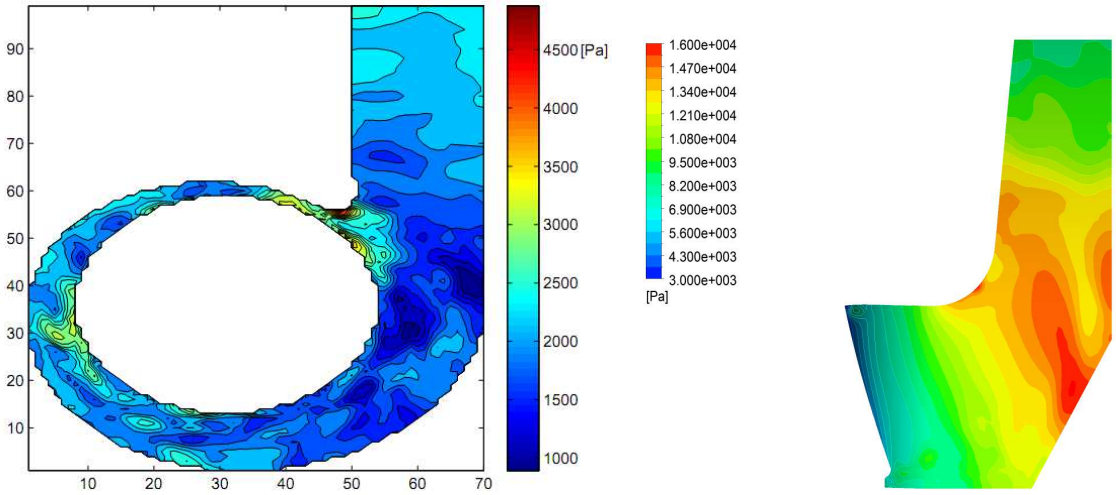

Figure 8: Amplitude of the pressure in volute and the impeller passage (spiral volute), 100% $\dot{m}_{opt}$

With the new configuration the impeller tongue interaction decreases, the pressure fluctuations in both domains are strongly reduced, especially in the blade channel. Figure 9 represents the results. Therefore it is interesting to know the behaviour of the new configuration under off-design conditions. Further results for the part load and over load conditions are visualized in figure 10 and figure 11.

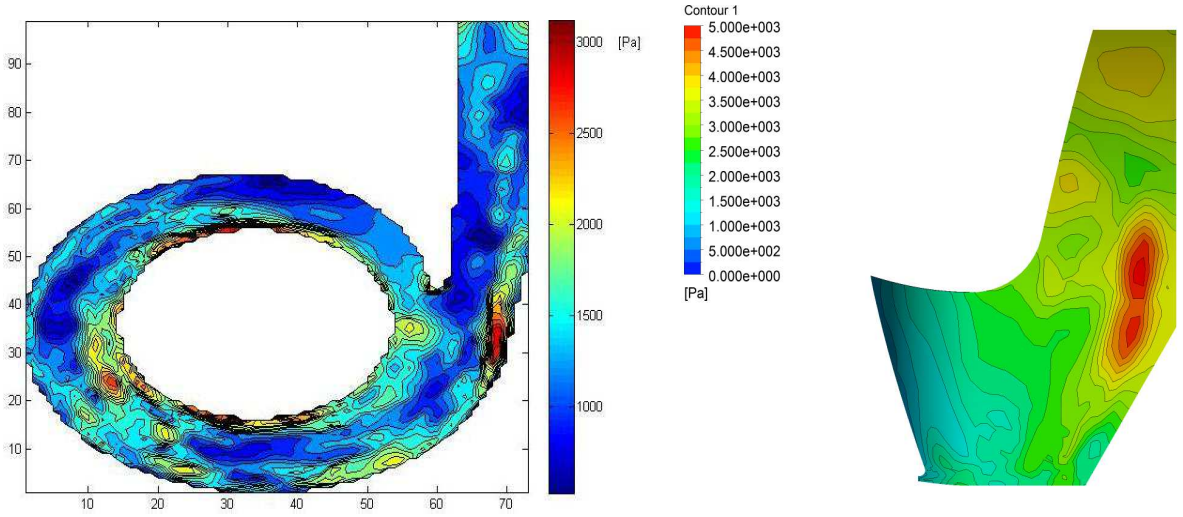

Figure 9: Amplitude of the pressure in volute and the impeller passage (with diffuser and collection volute), 100% $\dot{m}_{opt}$

The smallest pressure fluctuations occur at the design point. Due to the complex geometry of the blade channel, the pressure fluctuation reaches the highest amplitude in the region where the flow changes its direction from axial to radial. It decays further downstream of the flow. Amplitudes are much higher in the rotor compared to the volute.

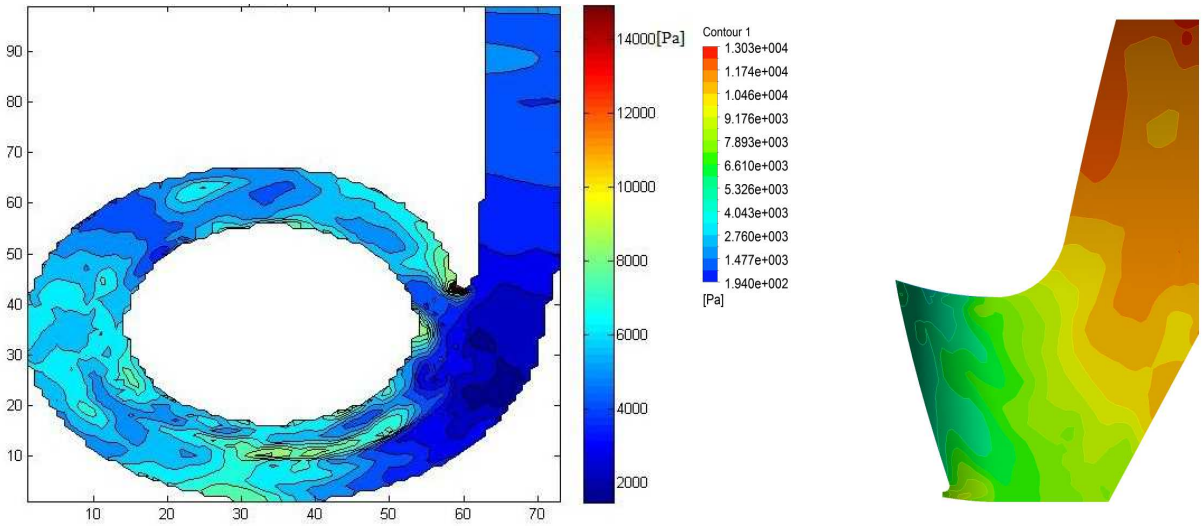

Figure 10: Amplitude of the pressure in volute and impeller passage (with diffuser and collection volute), 50% $\dot{m}_{opt}$

At the part load condition 50% of optimal flow rate, the maximum level of the pressure fluctuation in the impeller and volute is comparable. The diffuser effect in both impeller and volute escalates with decreasing flow rate. Therefore the instability affected by leading edge separation is enforced. The pressure fluctuation rises. The numerical simulation shows strong fluctuations at the outlet of the impeller and part of the shroud side. Compared to the amplitude of pressure fluctuation at design point, here the amplitude is almost 3 times higher. Because of a decreased radial velocity, the flow approaches the tongue with incorrect angle from the right side. The flow separates after the tongue and causes a strong fluctuation. The simulation shows increasing amplitude at the outlet of the vaneless diffuser with expanding cross section.

At overload conditions the fluctuation in the impeller is much stronger than in the volute. Figure 6 shows the contours of pressure amplitude. Similar to the part load situation, the pressure fluctuations increase at the tongue and the outlet of the vaneless diffuser. Compared to the part load condition the flow has weaker instability in the volute. In the impeller the flow at overload conditions cannot follow the shroud geometry, which causes separation at the shroud curvature and leads to strong pressure fluctuation.

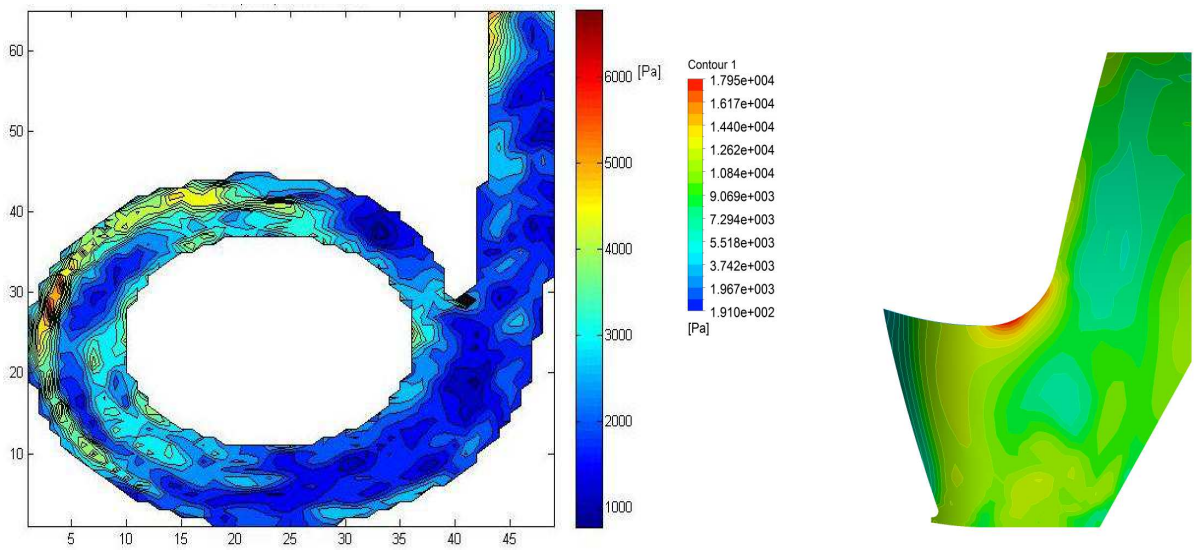

Figure 11: Amplitude of the pressure in volute and impeller passage (with diffuser and collection volute), 150% $\dot{m}_{opt}$

CONCLUSIONS

Two configurations of industrial ventilators were simulated in order to investigate fluctuation of pressure and to assess structural modification to eliminate these fluctuations. The application of a diffuser with collection volute reduced the amplitude strongly at design point. The amplitude and predominant frequency depend on the flow rate. The results obtained show strong pressure fluctuations in the impeller with impeller volute interaction. The pressure fluctuations are decaying from impeller to volute. At optimal and overload condition, the high pressure fluctuation is caused mainly by the redirection of the flow from axial to radial, e.g. the curvature at the shroud or the angle on hub. At part load conditions, because of the high diffuser effect in the impeller, strong pressure fluctuations occur at the outlet. A big diffuser outlet diameter reduces the impeller volute interaction. However, further simulations for the impeller are required in the future to determine the influence on the pressure fluctuation in the impeller.

ACKNOWLEDGEMENT

This work was funded by ZIM (Zentrales Innovationsprogramm Mittelstand), Germany, grant number KF2168201VT9. The computations have been run on the supercomputer HLRN-II of the North-German Supercomputing Alliance (HLRN, www.hlrn.de). Data of the radial fan as well as inspiring discussions have been provided by Piller Industrial Fans GmbH, Germany. The authors would like to thank all institutions for their kind support of this investigation.

BIBLIOGRAPHY

[1] F.R. Menter, M. Kuntz, R. Bender – *A Scale-Adaptive Simulation Model for Turbulent Flow Predictions.* AIAA Paper, **2003**

[2] A. Lucius, G. Brenner – *Unsteady CFD Simulations of a Pump in Part Load Conditions Using Scale-Adaptive Simulation*. Journal of Heat and Fluid Flow, 31, pp. 1113-1118, **2010**

[3] P. Chen, M. Soundra-Nayagam, A.N. Bolton, H.C. Simpson – *A Study of the inlet vortex in a centrifugal fan.* 11th Australasian Fluid Mechanics Conference, Hobart, Australia, **1992**

[4] P. Chen – *Unstable flow in centrifugal fans.* Journal of fluids engineering, Vol. 118, pp. 128-133, **1996**

[5] J. Feng, F.K. Benra, H.J. Dohmen – *Numerical Investigation on Pressure Fluctuations for Different Configurations of Vaned Diffuser Pumps.* International Journal of Rotating Machinery, **2007**

[6] S. Khelladi, C. Sarraf, F. Bakir, R. Rey – *Study of a high rotational speed shrouded centrifugal fan: aerodynamics and effects of a shroud-associated cavity on the performance.* J. Power and Energy, Vol. 224 **2010**

[7] W.K. Ng, M. Damodaran – *Computational Flow Modeling For Optimizing Industrial Fan Performance Characteristics.* European Conference on Computational Fluid Dynamics, Netherlands, **2006**

[8] R. Ballesteros-Tajadura, S. Velarde-Suarez, J.P. Hurtado-Cruz, C. Santolaria-Morros – *Numerical Calculation of Pressure Fluctuations in the Volute of a centrifugal Fan.* Journal of Fluids Engineering, Vol. 128, March **2006**

[9] K. Majidi – *Numerical Study of Unsteady Flow in a centrifugal Pump.* Journal of Turbomachinery, Vol. 127, April **2005**

[10] S. Madhavan, T. Wright – *Rotating Stall caused by Pressure Surface Flow Separation on Centrifugal Fan Blades.* Journal of Turbomachinery, Vol. 107, Issue 3, July **1985**